The Dynamical Relationship between Subtropical and Eddy-Driven Jets

SUKYOUNG LEE

Department of Meteorology, The Pennsylvania State University, University Park, Pennsylvania

HYUN-KYUNG KIM

Climate Prediction Center, National Centers for Environmental Prediction, Camp Springs, Maryland

(Manuscript received 14 May 2002, in final form 17 January 2003)

ABSTRACT

This study examines the impact of a subtropical jet on the development of baroclinic waves and polar-front jets with an idealized multilevel primitive equation model. Linear stability analysis and initial-value approaches suggest that baroclinic wave growth is most favored along the subtropical jet only when this jet is sufficiently strong. For a subtropical jet of modest strength, the most favorable region for baroclinic wave growth often lies 20° to 30° poleward of the subtropical jet, establishing an eddy-driven jet that is latitudinally well separated from the subtropical jet.

1. Introduction

Among the major features of the planetary-scale atmospheric general circulation, the quasi-zonal jets in the upper troposphere are of primary interest. It is well known that there are two different types of atmospheric jets: the subtropical jet and the polar-front or eddy-driven, jet. The subtropical jet is driven by angular momentum transport from the deep Tropics. This transport is accomplished through the Hadley cell, which, in part, is driven by thermal convection and radiative heating in the Tropics. While the observed tropical circulation is far from being zonally symmetric, the essential driving mechanism of the subtropical jet can be understood in the context of an eddy-free, axially symmetric flow. The axially symmetric circulation theory of Held and Hou (1980) features a subtropical jet centered at the poleward boundary of the Hadley cell (see the schematic picture in Fig. 1a).

In contrast to the thermally driven subtropical jet, jets can also be driven by baroclinic eddies. Examples of such jets can be found in the studies of Williams (1979), Panetta and Held (1988), Panetta (1993), and Lee (1997). The two-layer quasigeostrophic models on the β plane used in these studies neither support a subtropical jet, nor are they forced by a prescribed jet. Instead, the model flow is driven by a broad zone of uniform baroclinicity. When this flow is perturbed, baroclinic waves spontaneously grow, and meridional convergence of these baroclinic waves' westerly momentum flux then drives westerly jets. Thus, in these models, the eddy-free state is also jet-free. These model results demonstrate that in the absence of a preexisting jet, the eddies are capable of spontaneously generating a jet.

In the atmosphere, given the tendency of baroclinic eddies to drive jets, because these baroclinic eddies are most active in midlatitudes, one expects a jet driven by eddies to form in midlatitudes. This jet is the so-called polar-front or eddy-driven jet. This concept is illustrated in Fig. 1b. Also depicted in this figure is the meridional propagation of baroclinic waves and the mean meridional circulation driven by these waves' momentum and heat fluxes. However, this picture does not hold up for the *zonal-mean* flow during the NH winter where there is only one tropospheric jet centered at 30°N (e.g., see Fig. 7.5 in Peixoto and Oort 1992).

One possibility that can explain this difference is simply, for the NH winter, the region of strongest baroclinicity is collocated with that of the subtropical jet, and thus the primary growth of the baroclinic waves simply takes place at the same latitude as the preexisting subtropical jet (e.g., see Lindzen 1993; Sun and Lindzen 1994; Grotjahn 1993; Becker et al. 1997). In particular, Grotjahn (1993) states, ''Regions where the subtropical jets are strong are areas most favorable for cyclone storm development by the baroclinic instability process.'' This possibility is illustrated in Fig. 1c. Note that the extratropical mean meridional circulation is not indicated in this figure as its anticipated structure is not immediately obvious.

On the other hand, accounts of the jets made by some early investigators paint a picture that is consistent with the double jet flow shown in Fig. 1b. Palmén and New-

Corresponding author address: Dr. Sukyoung Lee, The Pennsylvania State University, 503 Walker Bldg., University Park, PA 16802.
E-mail: sl@essc.psu.edu

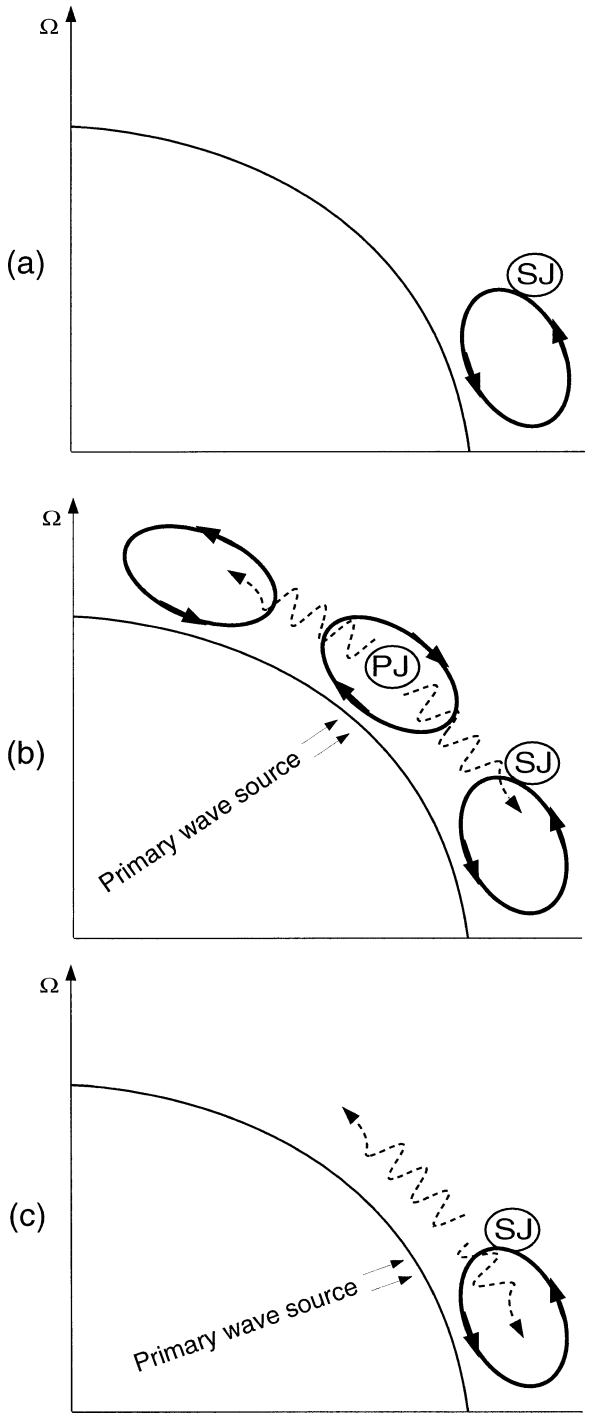

FIG. 1. Schematic diagrams for (a) axisymmetric circulation and zonal mean circulation of nonaxisymmetric flows when maximum baroclinic growth is at (b) midlatitudes and (c) the subtropical jet.

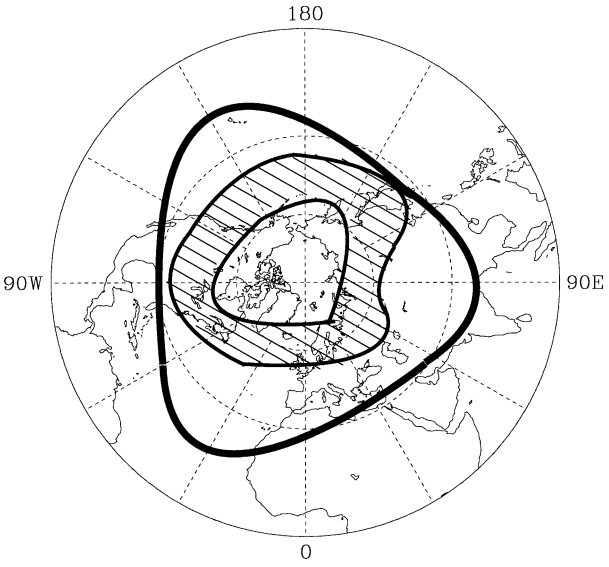

FIG. 2. Mean position of the subtropical jet (thick solid line) and the region (shaded) of principal polar-front jet activity (after Riehl 1962).

ton (1969) note, ''The strongest mean winds are observed at quite low latitudes, whereas the strongest baroclinicity, in the region of the polar front, is at a given time to be found at a considerably higher latitude around most of the hemisphere.'' Indeed, a schematic diagram of the NH winter jet stream, illustrated originally by Riehl (1962) and later by Palmén and Newton (1969), exhibits a general characteristic that is consistent with Fig. 1b. A reproduction of their schematic diagram is shown in Fig. 2.

If one examines Fig. 2 more closely, however, both processes described in Figs. 1b and 1c seem to take place at different longitudes. In this figure, one notices that the ridges and troughs of the subtropical and polar-front jets are out of phase; in regions where the subtropical jet forms at a relatively lower latitude (and is presumably weak), an eddy-driven jet forms at a much higher latitudes, and vice versa. As a result, in regions where the subtropical and the polar-front jets come close to each other, one expects to see a single maximum in the zonal wind, while in regions where these two jets are well separated, a double maxima may be seen. These characteristics are indeed hinted at in the NH winter climatological flow (e.g., see Fig. 7.14 in Peixoto and Oort 1992; Fig. 6.2 in Holton 1992). Most notably, between 120°E and 180° where the subtropical jet and polar-front jet come together (Fig. 2), one finds the strong Pacific jet centered at 35°N, and there is no apparent separate polar-front jet poleward of the Pacific jet. In contrast, between 60°W and 20°E, there are clearly two jets; a weak subtropical jet between 15°–20°N and the polar-front jet between 45°–55°N.

The aim of this study is to address the above two seemingly conflicting views—one that the strongest eddy generation takes place at the subtropical jet, and the other that the strongest eddy generation exists at latitudes considerably higher than the subtropical jet. Figure 2 hints that both views may be correct, but in different flow regimes; the first view may be correct

when the subtropical jet is strong and poleward intruding, while the second may be correct when the subtropical jet is weak and lies at a relatively low latitude. To examine this issue, we will use an idealized multilevel primitive equation (PE) model on the sphere in which we are able to systematically vary the strength of the subtropical jet. Following the above speculation, we specifically ask what impact the subtropical jet has on the development of the baroclinic eddies, and thus on the eddy-driven jet. This, of course, is not to say that the impact of baroclinic eddies on the subtropical jet is unimportant or negligible. It is well known that equatorward propagating eddies act to damp the subtropical jet (Palmén and Newton 1969; Held and Phillips 1990). The resulting ''wave drag'' can play a major role in driving the Hadley cell (Kim and Lee 2001b), and also can alter subsequent wave propagation by mixing potential vorticity. As such, the relationship among the subtropical jet, baroclinicity, baroclinic eddies, and eddy-driven jets is inherently nonlinear and complex. However, as alluded to above, a comprehensive investigation of these complex nonlinear interactions is beyond the scope of this study. The limitations of this study will also be discussed in section 6.

Section 2 briefly describes the numerical model used in this study, and explains the experimental design of this numerical model and the general analysis approach. The main results from the numerical model experiment are described in section 3. The conclusions follow in section 4.

2. Experiments, analysis approach, and model

a. Experimental design

We design numerical experiments that allow us to address the question raised above: How do the baroclinic waves and polar-front jets develop in the presence of a subtropical jet of various strengths? The question of how baroclinic eddies evolve and how they, in turn, modify the zonal mean flow is not new (e.g., Simmons and Hoskins 1978, 1980; Feldstein and Held 1989; Barnes and Young 1992; Gutowski et al. 1992; Thorncroft et al. 1993). The question that we would like to address here, however, is rather conceptual in that we first suppose that there exists an eddy-free, axially symmetric circulation driven by, say, an axially symmetric meridional gradient of diabatic heating (e.g., see Held and Hou 1980; Lindzen and Hou 1988). Such a flow consists of a Hadley cell and a subtropical jet, and is different from the initial state that previous studies of baroclinic life-cycles employed; in these studies, the initial flow is chosen, presumably based on observed flows for which the eddies already have modified the zonal mean flow. Instead, we ask how baroclinic waves will develop from a hypothetical axisymmetric state and how these waves modify this state. While this has not been investigated, the question was previously posed by Schneider and Lindzen (1977).

Accordingly, we first acquire a set of steady, eddy-free, axially symmetric states by integrating the axisymmetric version of a numerical model forward in time. In doing so, we design the model so that the subtropical jet strength is systematically varied, while the baroclinicity in the extratropical regions is held fixed. This is accomplished by systematically varying the amplitude of the tropical ''convective'' heating[1] Q_c [see Eq. (2) below], while keeping the radiative equilibrium temperature profile [see Eq. (1) below] fixed. Because Q_c is confined to the Tropics, as Q_c is varied, the baroclinicity in the extratropics, as measured by the Eady growth rate[2] changes very little in the axisymmetric circulations (cf. Figs. 3a–d).

Once an axisymmetric circulation is obtained, the meridional wind is set to zero, and a zonal wind field that nonlinearly balances the temperature and surface pressure fields is obtained (Branscome et al. 1989). The modification of the zonal wind resulting from obtaining the balanced state is very small as can be seen, for example, by comparing the zonal wind fields in Fig. 3a to that in Fig. 4a. (Note that the gray scale in these two figures differs from each other.) Taking this balanced state as an initial condition, a small-amplitude wave perturbation is introduced to the flow.

b. Analysis approach

This study makes extensive use of the unstable normal modes that arise from a linear stability analysis. This approach can be objected to on the grounds that it is highly unlikely that any single unstable normal mode can adequately describe observed baroclinic waves, and that a linear stochastic model approach, which takes into account a much broader wave spectrum, has been shown to be successful in various large-scale atmospheric and oceanic applications (e.g., Pendland and Sardeshmukh 1995; Whitaker and Sardeshmukh 1998; Zhang and Held 1999; Cash and Lee 2001).

While proven to be extemely useful for providing insight into various dynamical processes, and also as a forecasting tool, a linear stochastic model does not seem to be appropriate for the present study. The reason is that the axisymmetric state, which is our base

[1] The strength of the subtropical jet can also be controlled by the radiative equilibrium temperature profile. As demonstrated by Lindzen and Hou (1988), at least in the context of an axisymmetric solution, the subtropical jet position and strength are extremely sensitive to the latitude of the maximum heating rate. However, we do not feel that this approach is essential, as our aim is not to simulate the observed NH winter circulation, but to test the hypothesis; the essential factor that controls baroclinic wave development and the polar-front jet is the strength of the subtropical jet, not whether the strength is controlled by additional heating symmetric about the equator, or by off-equatorial maximum heating.

[2] We define Eady growth rate as a linear growth rate of the most unstable baroclinic normal mode, adapted from Eady's model (Eady 1949). The Eady growth rate takes the form of $0.3098(f/N)dU/dz$, where f is the Coriolis parameter, N the static stability, and U the zonal wind.

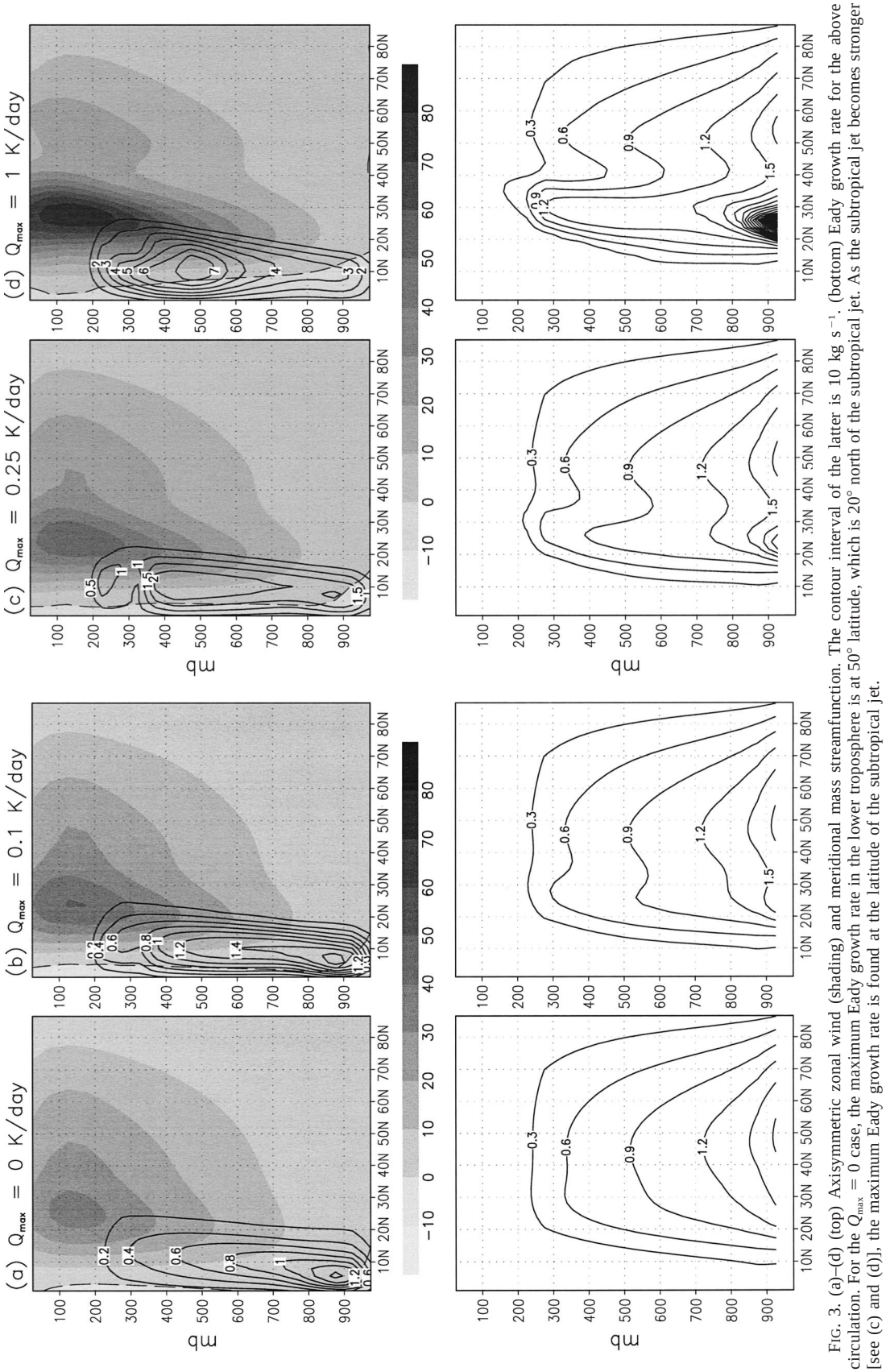

FIG. 3. (a)–(d) (top) Axisymmetric zonal wind (shading) and meridional mass streamfunction. The contour interval of the latter is 10 kg s^{-1}. (bottom) Eady growth rate for the above circulation. For the $Q_{max} = 0$ case, the maximum Eady growth rate in the lower troposphere is at 50° latitude, which is 20° north of the subtropical jet. As the subtropical jet becomes stronger [see (c) and (d)], the maximum Eady growth rate is found at the latitude of the subtropical jet.

state, is very unstable. For example, the growth rate of the most unstable normal mode for one of our basic states is 1.5 day^{-1} (also see the Eady growth rates in Fig. 3). To construct a linear stochastic model for such a highly unstable flow, we will need to add a very large amount of damping to stabilize the system. If one is to employ uniform damping as in many other studies, we are uncertain as to what physical processes such a strong, uniform damping represents.[3] On the other hand, the use of nonuniform damping, which presumably can better tune the stochastic model, seems to be rather contrived. Thus, we feel that the use of linear stability analysis, although perhaps not ideal, remains as a viable approach, as long as the results are interpreted with care. The benefit of linear stability analysis can be seen a posteriori; it will be shown that latitude of the maximum amplitude of the normal mode coincides with that of the maximum baroclinicity, the maximum eddy momentum flux convergence, and the eddy-driven jet maximum of the baroclinic life cycle calculations.

c. Model description

The model used in this paper is based on the dynamical core of the Geophysical Fluid Dynamics Laboratory (GFDL) general circulation model (Gordon and Stern 1982). Because the model parameterizations adopted in this study are described in Kim and Lee (2001a, 2001b), only a brief description of the model and parameterizations are provided here.

The horizontal resolution is rhomboidal 30, and there are 20 equally spaced sigma levels. The model is driven by thermal relaxation toward a ''radiative–convective'' equilibrium temperature profile similar to that used by Held and Hou (1980), except that at levels above the model's tropopause, the sign of the meridional gradient of the equilibrium temperature is reversed:

$$T_E(\theta, \sigma) = \Theta_E \sigma^\kappa = \Theta_0 \sigma^\kappa \left\{ 1 - \frac{1}{3}\Delta_h [3(\sin\theta - \sin\theta_0)^2 - 1] - \Delta_v \left(\frac{h}{H} \ln\sigma + \frac{1}{2} \right) \right\}, \quad \text{for } 0.2 < \sigma < 1 \tag{1a}$$

$$T_E(\theta, \sigma) = T_E(\theta = 90^\circ\text{N}\ \sigma = 0.225) + 60\ \text{K} \quad \text{for } \sigma = 0.175 \tag{1b}$$

$$T_E(\theta, \sigma) = T_E(\theta, \sigma = 0.175) - \frac{1}{2}\Delta T \frac{1}{3} \cos^2(\theta - \theta_0), \quad \text{for } \sigma = 0.125 \tag{1c}$$

$$T_E(\theta, \sigma) = T_E(\theta, \sigma = 0.175) - \Delta T \frac{1}{3} \cos^2(\theta - \theta_0), \quad \text{for } \sigma = 0.075 \tag{1d}$$

$$T_E(\theta, \sigma) = T_E(\theta, \sigma = 0.175) - \frac{1}{2}\Delta T \frac{1}{3} \cos^2(\theta - \theta_0), \quad \text{for } \sigma = 0.025, \tag{1e}$$

where θ is latitude; Θ_E is the radiative–convective equilibrium potential temperature; $\kappa = R/c_p$ (R is the gas constant, and c_p is the specific heat at constant pressure); Θ_0 is the tropospheric global mean value of Θ_E; ΔT is the temperature difference between the pole and the equator; Δ_h and Δ_v are the fractional change in Θ_E from the equator to the pole; and from the tropopause to the surface, respectively, and h and H are the scale height and the tropopause height, respectively. As can be seen in (1b)–(1e), at levels above the model's tropopause, the meridional gradient of Θ_E is reversed so that the zonal mean zonal wind decreases with height. The model parameters are fixed as $h = 8.0 \times 10^3$ m, $H = 1.0 \times 10^4$ m, $\Theta_0 = 300$ K, $\Theta_0\Delta_v = 12.5$ K, and $\Theta_0\Delta_h = 60$ K.

[3] Such concern was not an issue in previous linear stochastic model studies, as the linear operator of the model was derived, in one form or another, from the time-mean state of a fully nonlinear flow. Thus, to construct such a stochastic model, only a moderate amount of damping needs to be added to the system to suppress any exponentially growing modes. This added damping is often interpreted as representing the nonlinear effect of the perturbations as well as the friction.

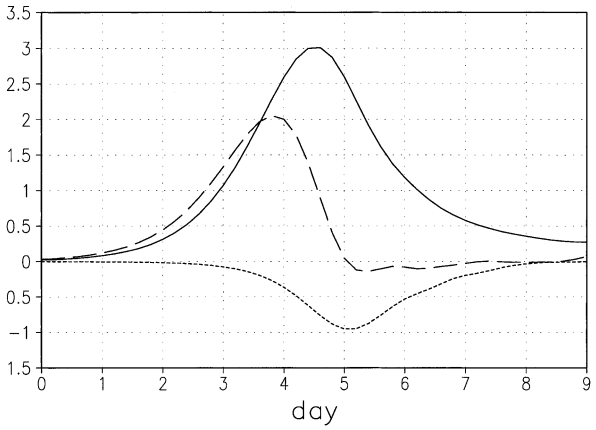

FIG. 4. Time evolution of the total eddy energy (solid line), the baroclinic energy conversion (dashed line), and the barotropic energy conversion (dotted line) for the $Q_{max} = 0$ case. The total eddy energy is normalized by 1×10^4 J m^{-2}, and the energy conversions are normalized by 1×10^4 J m^{-2} day^{-1}.

The model is also forced by an additional constant heating Q_c, which is used to crudely represent convection in the Tropics (Becker et al. 1997; Kim and Lee 2001b):

$$\frac{Q_c}{Q_{\max}} = \begin{cases} \exp\left[-\dfrac{(p - p_0)^2}{2\sigma_p^2}\right] \times \cos^2\left[\dfrac{\pi}{2}\left(\dfrac{\theta - \theta_0}{\sigma_\theta}\right)\right] & \text{for } |\theta - \theta_0| < \sigma_\theta \\ 0 & \text{otherwise,} \end{cases} \tag{2}$$

where $Q_{\max} = 2$ K day^{-1}, $p_0 = 525$ mb, $\sigma_p = 200$ mb, $\theta_0 = 0°$ and $\sigma_\theta = 20°$. As motivated in the previous section, this additional tropical heating is included to control the strength of the subtropical jet while keeping the midlatitude baroclinicity relatively intact.

The steady-state solutions of the zonally symmetric version of the above model are used as initial conditions for the nonlinear eddy life cycle calculations. Since it is necessary to include vertical diffusion of momentum for the axisymmetric flows, the model includes vertical diffusion of momentum and heat. The detailed description of these damping terms is provided in Kim and Lee (2001a). The value of the biharmonic horizontal diffusion coefficient used in the eddy life-cycle calculation is 1×10^{17} m^4 s^{-1}.

3. Results

Upper pannels in Figs. 3a–d show the steady-state, axisymmetric circulation's zonal wind and meridional mass streamfunction for $Q_{\max} = 0$ K day^{-1}, 0.1 K day^{-1}, 0.25 K day^{-1}, and 1.0 K day^{-1}, respectively. The lower panels of each figure show the Eady growth rate. As expected from the theory of axisymmetric circulations, in all four cases, the poleward end of the Hadley cell, as can be inferred from the meridional mass streamfunction, coincides with the subtropical jet (Schneider 1977). Also, as the value of $Q_{\max}$ increases, the subtropical jet strengthens and shows a hint of poleward migration.

While only slightly hinted at in Fig. 3a, there are two branches of maximum Eady growth rate, one along the subtropical jet (subtropical branch, hereafter) and the other in the midlatitudes (midlatitude branch, hereafter). For the case of $Q_{\max} = 0$ K day^{-1}, shown in Fig. 3a, while the subtropical jet is at 25° latitude, the Eady growth rate peaks near 50° latitude where there is no preexisting jet. As the value of $Q_{\max}$ increases, the maximum Eady growth rate moves from midlatitudes to the latitude of subtropical jet; for $Q_{\max} = 0.1$ K day^{-1}, there are two comparable maxima in the Eady growth rate, one near 50° and the other at 25°; for $Q_{\max} = 0.25$ K day^{-1}, the primary peak occurs at 25°, and this feature is further accentuated for $Q_{\max} = 1.0$ K day^{-1}. As will be shown below, the latitude at which the amplitude of the most unstable normal mode peaks is indeed consistent with the above Eady growth rate distribution.

For all of the above cases, when the initial axisymmetric flow is perturbed with a small-amplitude disturbance, the most unstable normal mode undergoes baroclinic growth followed by barotropic decay. As an example, in Fig. 4, we show the time evolution of the total eddy energy, baroclinic growth, and barotropic decay of the most unstable zonal wavenumber 6 normal mode for the case of $Q_{\max} = 0$ K day^{-1}. Throughout this paper, day 0 is defined as the day that the growth rate starts to deviate from the linear growth rate. The maximum barotropic energy conversion from the wave to the zonal mean flow occur about 1.5 days after the baroclinic energy conversion peaks. This is similar to the results of previous baroclinic life-cycle studies in which the midlatitude jet is already built into the initial flow (e.g., Simmons and Hoskins 1978, 1980; Feldstein and Held 1989; Barnes and Young 1992; Thorncroft et al. 1993).

a. An example of the flow evolution under a "weak" subtropical jet

Figures 5a–d display four snapshots of zonal winds and Eliassen–Palm (EP) flux vectors (Edmon et al. 1980) for the case of $Q_{\max} = 0$ K day^{-1}, where the initial state is the axisymmetric state (see Fig. 3a), and the model days are in accord with the times shown in Fig. 4. Note that gray shading in Figs. 3, 5, and 8 are different from each other. Consistent with the Eady growth rate, the eddies start to grow centered at around 50°N, 25° poleward of the subtropical jet. In this midlatitude region, where the largest vertical component of the EP flux vector lies, the lower-level zonal mean zonal wind first increases, initiating the formation of the polar-front jet. In the upper troposphere, the EP flux vectors first start to turn equatorward, signifying a poleward flux of westerly eddy momentum. The result is that by day 5, the eddies fully establish the polar-front jet (Fig. 5d). Consistent with the Eady growth rate diagram, it can be seen that secondary baroclinic wave growth takes place in the region of subtropical jet.

While there is little doubt that this polar-front jet plays a role in organizing eddies that grow subsequently, this calculation demonstrates that the baroclinic eddies do not need to be organized by a preexisting jet (cf. Panetta

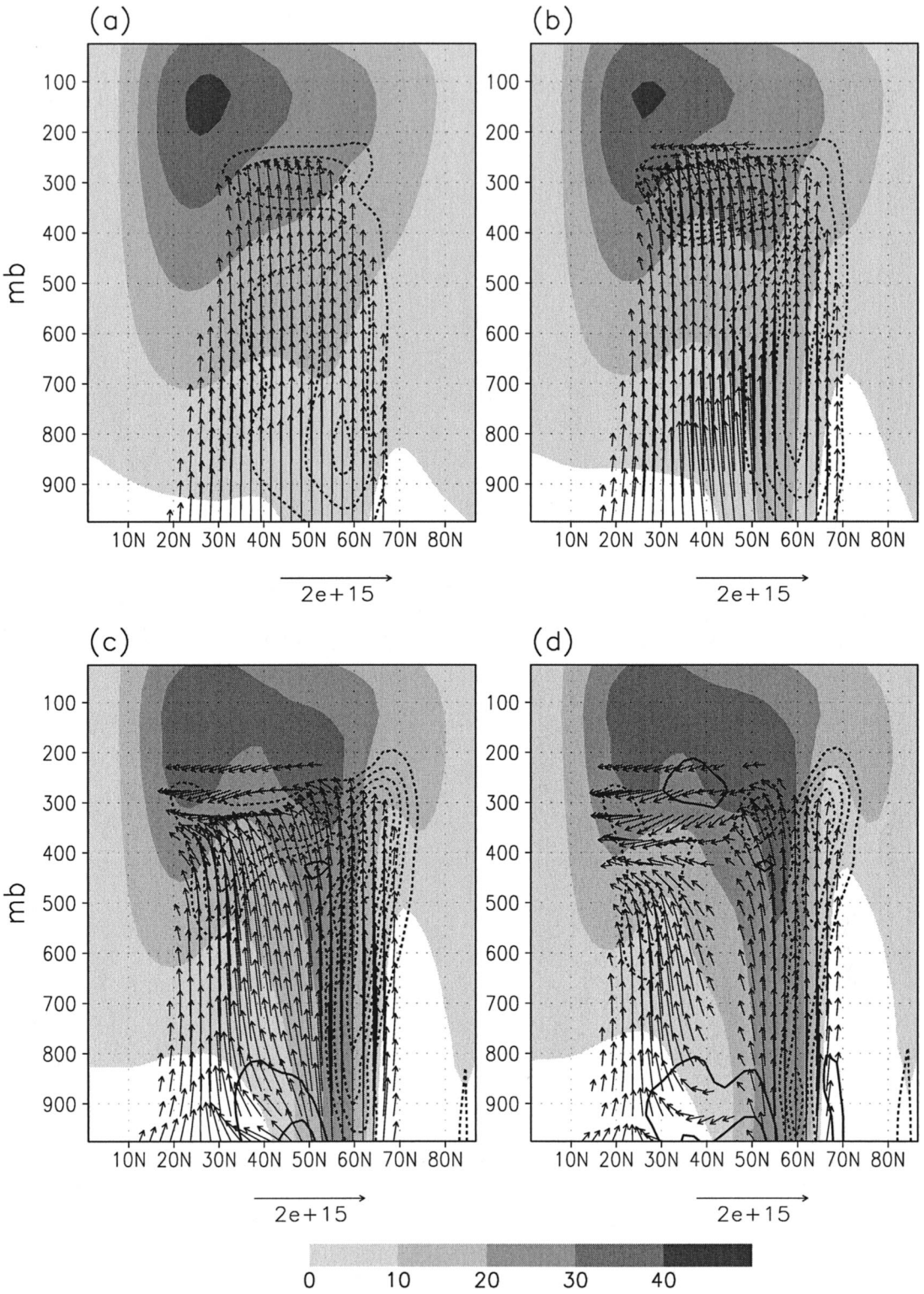

FIG. 5. Snapshots of zonal wind (shading), EP (vectors), and EP flux convergence (solid lines) and divergence (dashed lines) for the $Q_{max} = 0$ case. The contour interval is 2.5×10^{-4} m s^{-2}.

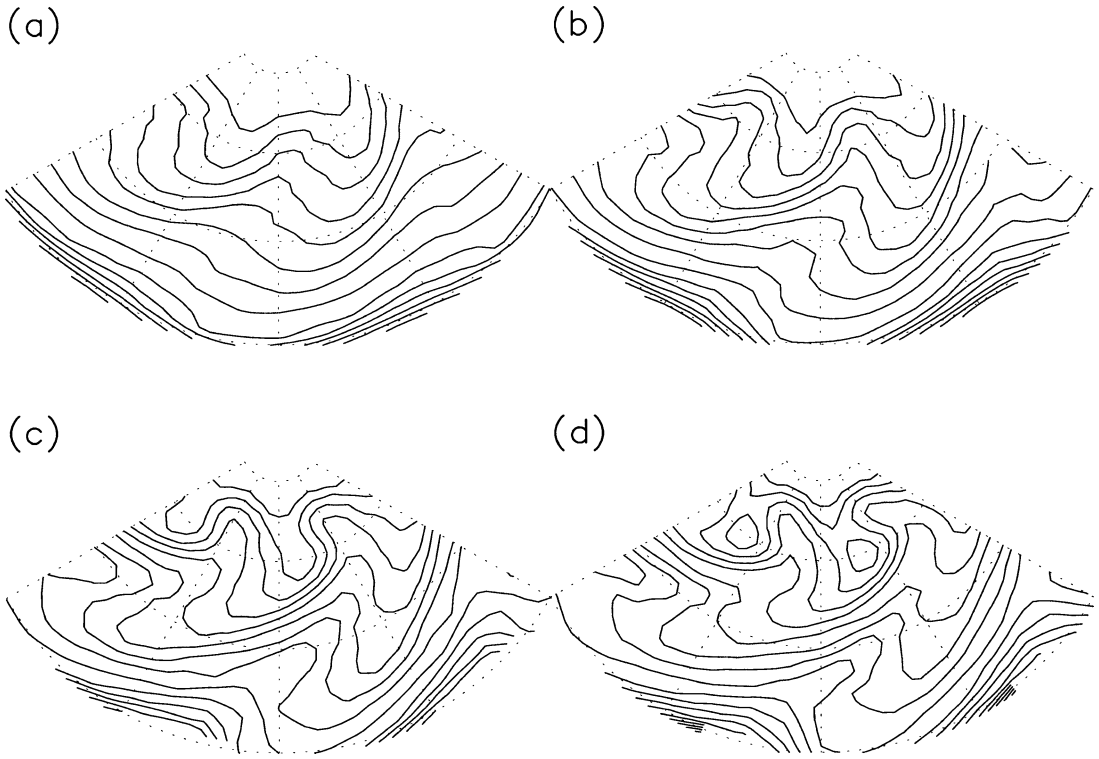

FIG. 6. Snapshots of potential temperature on 2-PVU surface for $Q_{max} = 0$ case corresponding to those shown in Fig. 5. Sectors are shown for two wavelengths. The contour interval is 5 K.

and Held 1988; Panetta 1993; Lee 1997). Moreover, this takes place even when there is a preexisting, subtropical jet. In other words, a subtropical jet does not necessarily organize baroclinic eddies. Essentially the same results are obtained for the cases of $Q_{max} = 0.05$, 0.1, 0.125, and 0.25 K day^{-1} for a range of zonal wavenumbers from 4 to 8 (not shown).

The horizontal structure of the wave is consistent with the occurrence of strong wave radiation in the meridional direction, as implied by the upper-tropospheric EP flux vectors. Figure 6 shows snapshots of the potential temperature field on the 2-potential-vorticity-unit (PVU; 1 PVU $= 10^{-6}$ m^2 s^{-1} K kg^{-1}) surface, the nominal tropopause, while Fig. 7 shows snapshots of the 300-mb eddy streamfunction field. Both fields show that, as the baroclinic wave matures, the wave becomes noticeably elongated in the meridional direction, with a strong horizontal tilt, indicative of meridional radiation.

b. An example of the flow evolution under a ''strong'' subtropical jet

In contrast to the relatively weak subtropical jet cases in subsection 3a, when the initial axisymmetric circulation in low latitudes is driven more forcefully so that a stronger subtropical jet arises (see Fig. 3d), a perturbation introduced to such a flow spontaneously evolves into growing baroclinic waves whose amplitude peaks at a latitude slightly poleward of the subtropical jet; they grow on the poleward side of the subtropical jet. This result is consistent with previous studies of baroclinic eddy life cycles on the sphere for which baroclinic waves tend to grow on the poleward side of an initial jet. The evolution shown in Fig. 8 indicates that baroclinic eddies are almost entirely organized by this subtropical jet.

In this strong subtropical jet case, there is one aspect of the wave evolution that is somewhat different from previous life cycle calculations. The EP flux vectors indicate that meridional radiation is extremely weak (Fig. 8). Indeed, the potential temperature on the 2-PVU surface (Fig. 9) shows essentially no meridional tilt during the entire course of the life cycle, and the barotropic energy conversion from the eddy to the mean flow is very weak (not shown). The 300-mb streamfunction fields (Fig. 10) show that the baroclinic eddies in this case are much more isotropic than those in the weak subtropical jet case. These characteristics suggest that the eddies in this strong subtropical-jet case may be meridionally trapped edge waves (Swanson et al. 1997). The eddies eventually decay through a rather complex second life cycle (not shown). In the second cycle, the eddies decay through both barotropic and *baroclinic* energy conversions. Such unusual behavior is not too surprising, given that the initial flow is much more unstable than flows considered in previous studies. This second life cycle is not closely examined, because it

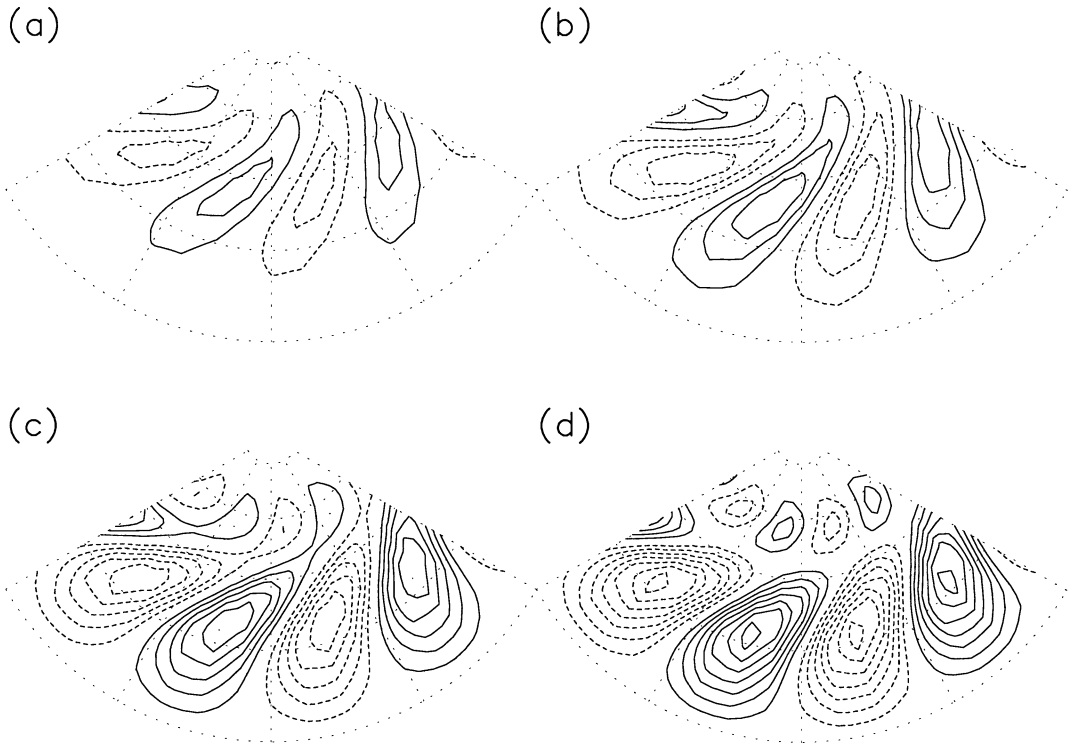

FIG. 7. Snapshots of streamfunction at 300 mb for $Q_{max} = 0$ case corresponding to those shown in Fig. 5. Sectors are shown for two wavelengths. The contour interval is 2×10^7 m^2 s^{-1}, and zero contours are omitted.

apparently is not relevant for either the long-time behavior of this model or for the atmosphere, since negative baroclinic energy conversion rarely occurs in the atmosphere.

At least in the dynamical framework of the eddy-zonal mean flow interaction, the above results indicate that the existence of a purely eddy-driven jet is controlled by the strength and latitude of the subtropical jet. In the presence of a strong subtropical jet, an eddy-driven jet of substantial strength does not form, whereas it does in a flow where the subtropical jet is weak.

c. Summary

Figure 11 summarizes this behavior by displaying the latitudes of the subtropical jet and corresponding eddy-driven jet. The latter is obtained from the most unstable $k = 6$ normal mode of the corresponding axisymmetric circulation. More precisely, the latitude of the eddy-driven jet displayed in Fig. 11 is defined as the latitude of the maximum eddy momentum flux convergence of the unstable normal modes; further details can be found later in this subsection. In all cases that we examined, the latitude of the maximum eddy momentum flux convergence, predicted by the unstable normal mode, coincides with that of the maximum baroclinicity. This latitude, as can be seen by comparing Figs. 3a and 5, successfuly predicts the central latitude of the nonlinear eddy momentum flux convergence obtained in the nonlinear life cycle calculation.

The results summarized by Fig. 11 tell us that as the subtropical jet strengthens and expands poleward,[4] the unstable normal mode predicts an abrupt transition from a double jets state—eddy-driven and subtropical jets coexisting together—to a state consisting of a single jet. This abrupt transition is hinted at by the Eady growth rate of the axisymmetric flow (Fig. 3). As the tropical thermal driving intensifies, the growth rate in the subtropical branch increases (compare Figs. 3a–d), and when this growth rate exceeds that of the midlatitude branch, the above abrupt transition takes place.

The above bifurcation also hints that even when the maximum amplitude of the fastest growing normal mode resides at the subtropical branch, there must exist either a secondary maximum along the midlatitude branch for the most unstable normal mode or another less unstable normal mode whose primary maximum amplitude lies at the midlatitude branch. It turns out that for the case of $Q_{max} = 0.5$ K day^{-1}, a secondary peak

[4] Because both the strength and latitude of the subtropical jet increase with the intensity of the heating, calculations presented here cannot discriminate the relative importance of the subtropical jet's strength and latitude on the formation of the eddy-driven jet. While in principle it is possible to design the experiments in such a way to separate the impact of the jet strength from that of the jet position, such calculations are not performed.

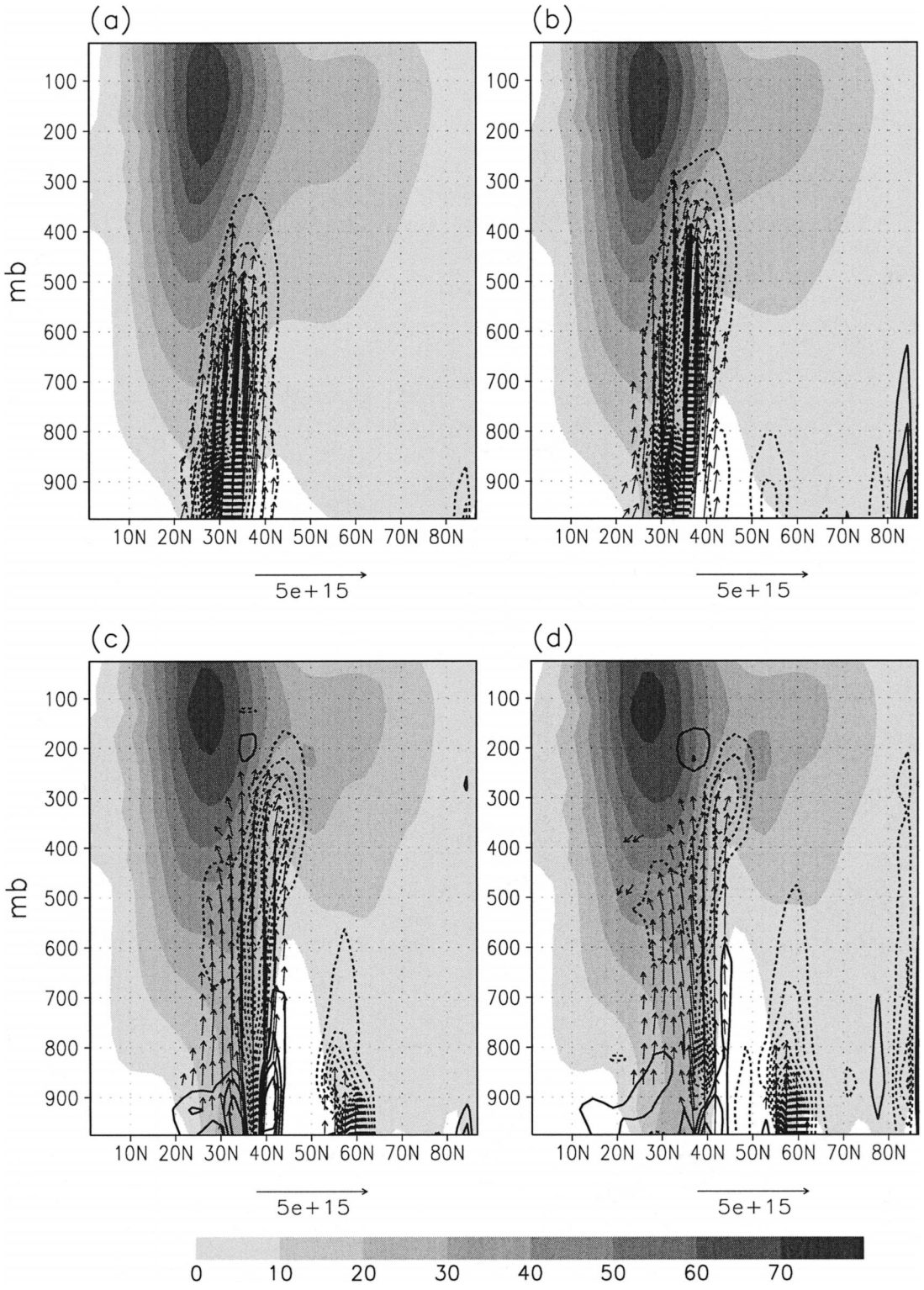

FIG. 8. Same as Fig. 5, except for the $Q_{max} = 1$ case.

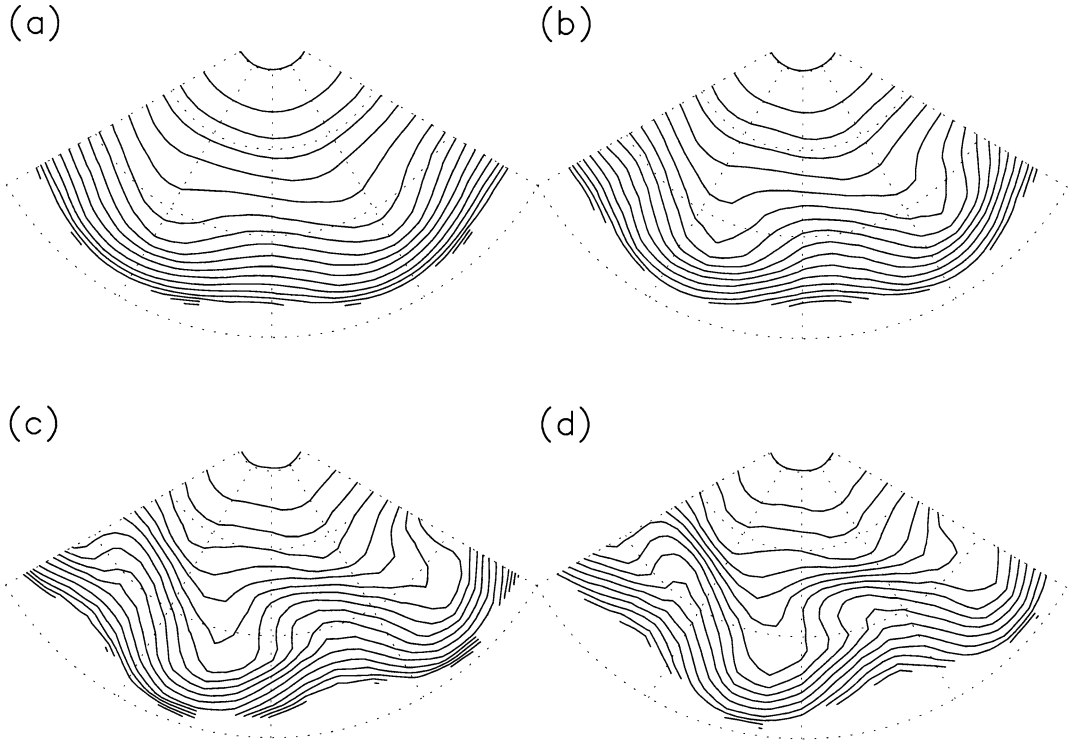

FIG. 9. Snapshots of potential temperature on 2-PVU surface for $Q_{max} = 1$ case corresponding to those shown in Fig. 8. Sectors are shown for two wavelengths. The contour interval is 5 K.

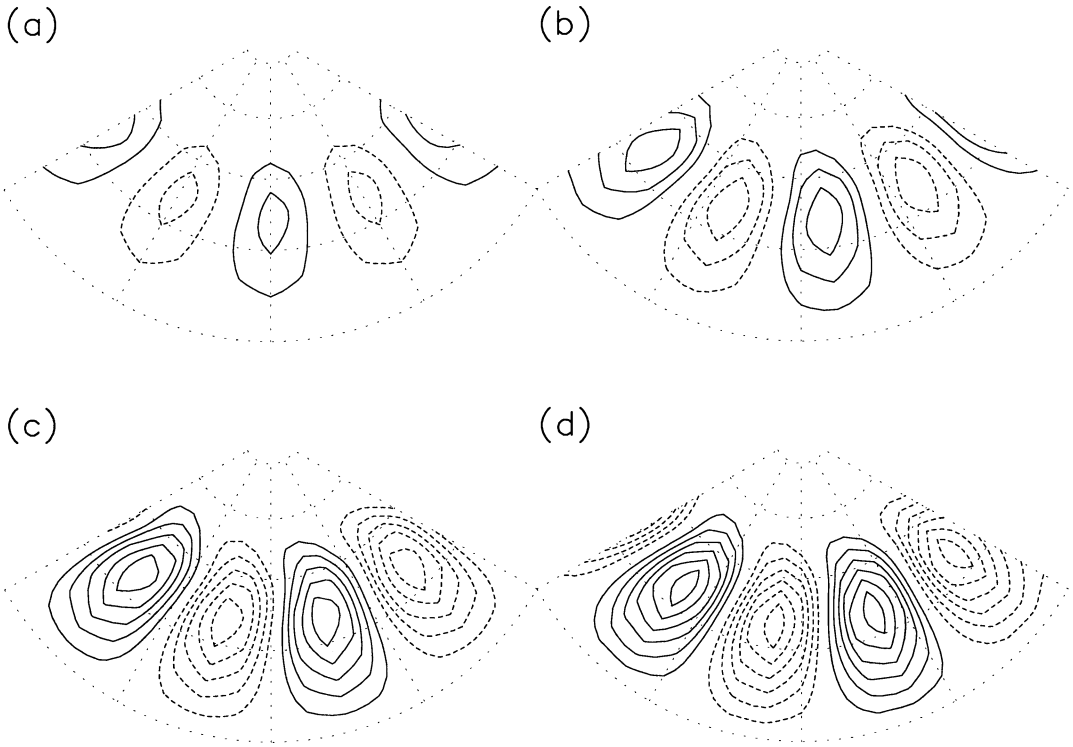

FIG. 10. Snapshots of streamfunction at 300 mb for $Q_{max} = 1$ case corresponding to those shown in Fig. 8. Sectors are shown for two wavelengths. The contour interval is 2×10^7 m^2 s^{-1}, and zero contours are omitted.

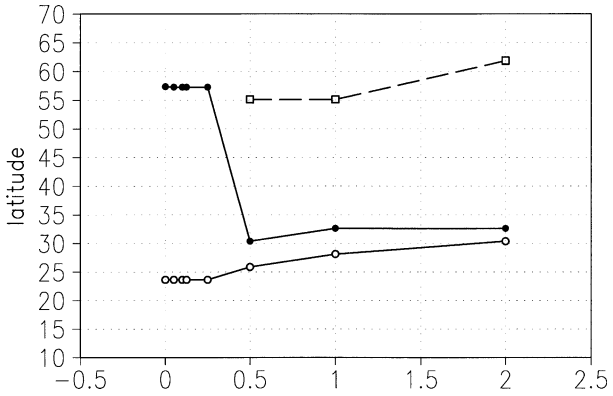

FIG. 11. Latitudes of both the subtropical jet (thick solid line), and the primary (thin solid line) and secondary (thin dashed line) positions of the eddy-driven jet. The latitudes of the eddy-driven jet are predicted with the unstable normal modes of an axisymmetric flow. See the text for more details.

appears at the midlatitude branch in the fastest growing normal mode. For the case of $Q_c = 1$ K day^{-1} and 2 K day^{-1}, the midlatitude peak appears in other normal modes with slower growth rates. These are indicated by the dashed line in Fig. 11. To this end, it needs to be stressed again that we attach no special meaning to the growth rate and the rank of the unstable normal modes. What should be noted instead is that for the flow under consideration, linear theory predicts two branches of baroclinic wave activity, one along the midlatitude (away from the subtropical jet) branch, and the other along the subtropical branch; the subtropical jet strength and its position determine the relative dominance of these two branches.

The qualitative behavior summarized by Fig. 11 is also valid for zonal wavenumbers 4–8 (not shown). For even smaller zonal wavenumbers, the maximum amplitude of the unstable normal modes tends to move closer to the subtropical jet. Given the limitations of the unstable normal mode approach as described above, however, a more detailed sensitivity analysis of the unstable normal modes seems unwarranted, and thus is not pursued further.

4. Conclusions

At least in the idealized numerical model experiment, the existence of an eddy-driven jet is dictated by the strength and latitude of the subtropical jet. If a subtropical jet is sufficiently strong, the primary region of the baroclinic wave growth coincides with the region of the subtropical jet. As a result, a prominent polar-front jet does not form at latitudes much higher than the latitude of the subtropical jet. On the other hand, in the presence of a weak subtropical jet, baroclinic wave growth takes place primarily in the midlatitude baroclinic zone, establishing a well-defined polar-front jet at this latitude. This result shows that even in the earth-like parameter space, and on a spherical geometry, a preexisting jet is not always required for organizing the baroclinic eddies (cf. Williams 1979; Panetta and Held 1988; Panetta 1993). Without a preexisting jet, the eddies are able to spontaneously grow, and then to drive a jet. Moreover, this takes place even when there is a preexisting, subtropical jet.

The above model results (see Fig. 11 for summary) are not inconsistent with the out-of-phase relationship between the latitude of the subtropical and polar-front jets, as shown in Fig. 2; that a strong and more poleward-intruding subtropical jet coincides with a more equatorward eddy-driven jet, and that a weak and less poleward-intruding subtropical jet occurs with a more poleward eddy-driven jet at the same longitudinal sector.

While there is no doubt that the zonal asymmetry shown in Fig. 2 reflects the presence of stationary waves forced by topography and heating, the idealized model results suggest that the subtropical jet has an important impact on midlatitude baroclinic waves, and provides an alternative explanation for the features depicted in Fig. 2. In fact, one might argue that this latter perspective provides a basic framework for understanding the topographically forced stationary waves, by noting that these stationary waves require lower-level westerlies for their existence through the term $\mathbf{u}_H \cdot \nabla_H h_{\text{topo}}$, where $\mathbf{u}_H$ is the horizontal wind vector, and h_{topo} is the topographic height. Because the central latitude of the Tibetean Plateau is at 40°N and the Rockies extends mostly over middle and high latitudes, the lower-level westerlies that interact with these mountains to excite stationary waves must ultimately be driven by midlatitude baroclinic eddies. Thus, it seems logical to first ask how the low-level midlatitude westerlies are driven, and what determines the strength and position of these westerlies. The results of this study provides some insight into this question.

In light of the above argument, returning to the two conflicting views discussed in the introduction, we conclude that both views are correct but under different circumstances. The notion that the eddy generation is greatest along the subtropical jet is correct, but only in the regime where the subtropical jet is sufficiently strong. In the same token, the account of Palmén (1954) that the largest baroclinicity is at a latitude much higher than the subtropical jet is also correct, but only when the subtropical jet is not too strong and located at a relatively low latitude. In fact, Palmén (1954) tried to resolve the apparent inconsistency by recognizing that there are ''two separate wind systems, a steady subtropical jet stream and a polar front system that fluctuates in latitude and consequently does not so strongly influence the average winds at a given location.'' (Palmén and Newton 1969). However, unlike the main result of this study, this observation itself, insightful as it is, does not explain the out-of-phase relationship between the latitude of the subtropical and polar-front jets.

It should be noted that some of the details of the main

results summarized in Fig. 11 must be sensitive to the model specifications. For example, the precise threshold value for the strength and position of the subtropical jet that divides the ''weak subtropical jet regime'' from the ''strong subtropical jet regime'' must be sensitive to the static stability as well as the meridional temperature gradient specified by the radiative equilibrium temperature profile. It would be useful to develop an analytical theory that can identify a key parameter that accurately formulates the weak versus strong subtropical regime.

The main result of this study needs to be tested with statistically steady states. While the initial value approach adopted in this study is advantageous for examining the temporal evolution of the baroclinic eddies and zonal mean flow, in order to relate this study's main result to the general circulation characteristics of the atmosphere, the result needs to be supported by statistically steady states. In extending this study in that direction, it is crucial to include moist processes in the model. The reason is that eddy-induced midlatitude diabatic heating (Hoskins and Valdes 1990), while relatively unimportant during the initial stages of the flow evolution, can make a qualitative difference for equilibrium, statistically steady, zonal wind structures (e.g., Becker and Schmitz 2001; Kim and Lee 2002, manuscript submitted to *J. Atmos. Sci.*). In fact, our preliminary calculations of statistically steady states indicate that the two-jet structure of the weak subtropical jet regime becomes robust only when moist processes are included in the model. These preliminary calculations also indicate that the complexity that arises from nonlinear interaction between the subtropical jet and the midlatitude baroclinicity renders the statistically steady-state solution even more sensitive to the radiative equilibrium temperature profile than what linear theory predicts. This behavior calls for a more extensive, systematic testing of the main result reported in this study.

Notwithstanding the above limitations, the results of this study suggest that the Asia–Pacific sector falls into the strong subtropical jet regime, while the North Atlantic sector belongs to the weak subtropical jet regime (Thompson et al. 2002). This possibility has an interesting implication both for midlatitude storm tracks and for the North Atlantic Oscillation (NAO). It offers an hypothesis as to why a prominent NAO-like dipole occurs in the Atlantic sector, rather than in the Pacific sector, and why the amplitude of the Atlantic storm track is as large as its Pacific counterpart, in spite of the fact that the *time-mean* zonal winds and associated baroclinicity (e.g., see Hoskins and Valdes 1990) are much greater over the Pacific than the Atlantic. When the background potential vorticity (PV) gradient is very sharp, as for the subtropical jet over the western Pacific, Rossby waves propagating along that PV gradient are better described as meridionally trapped edge waves (Hoskins and Ambrizzi 1993; Swanson et al. 1997). For such waves, the meridional particle displacement, and hence the storm track amplitude, is expected to be relatively small. In contrast, in regions where there is a polar-front jet, as in the midlatitude North Atlantic, there is no ''externally'' imposed sharp PV gradient.[5] Therefore, one may expect relatively large particle displacements, and hence stronger storm track eddies. For the same reason, to the extent that the tropospheric NAO is driven by temporal fluctuation of baroclinic eddy fluxes, one expects variability to be larger in the North Atlantic.

Acknowledgments. We thank Dr. Steven Feldstein for his comments on this manuscript. Comments from two anonymous reviewers also improved this manuscript. Model calculations performed by S.-W. Son helped the revision of this manuscript. This research was supported by the National Science Foundation through Grant ATM-0001473.

REFERENCES

Barnes, J. R., and R. E. Young, 1992: Nonlinear baroclinic instability on the sphere: Multiple life cycles with surface drag and thermal damping. *J. Atmos. Sci.,* **49,** 861–878.

Becker, E., and G. Schmitz, 2001: Interaction between extratropical stationary waves and the zonal mean circulation. *J. Atmos. Sci.,* **58,** 462–480.

——, ——, and R. Geprägs, 1997: The feedback of midlatitude waves onto the Hadley cell in a simple general circulation model. *Tellus,* **49A,** 182–199.

Branscome, L. E., W. J. Gutowski Jr., and D. A. Stewart, 1989: Effect of surface fluxes on the nonlinear development of baroclinic waves. *J. Atmos. Sci.,* **46,** 460–475.

Cash, B. A., and S. Lee, 2001: Observed nonmodal growth of the Pacific–North American teleconnection pattern. *J. Climate,* **14,** 1017–1028.

Eady, E. T., 1949: Long waves and cyclone waves. *Tellus,* **1,** 33–52.

Edmon, H. J., B. J. Hoskins, and M. E. McIntyre, 1980: Eliassen–Palm cross sections for the troposphere. *J. Atmos. Sci.,* **37,** 2600–2616.

Feldstein, S. B., and I. M. Held, 1989: Barotropic decay of baroclinic waves in a two-layer beta-plane model. *J. Atmos. Sci.,* **46,** 3416–3430.

Gordon, C. T., and W. F. Stern, 1982: A description of the GFDL spectral model. *Mon. Wea. Rev.,* **110,** 625–644.

Grotjahn, R., 1993: *Global Atmospheric Circulations: Observations and Theories.* Oxford University Press, 430 pp.

Gutowski, W. J., L. E. Branscome, and D. A. Stewart, 1992: Life cycles of moist baroclinic eddies. *J. Atmos. Sci.,* **49,** 306–319.

Held, I. M., and A. Y. Hou, 1980: Nonlinear axially symmetric circulations in a nearly inviscid atmosphere. *J. Atmos. Sci.,* **37,** 515–533.

——, and P. J. Phillips, 1990: A barotropic model of the interaction between the Hadley cell and a Rossby wave. *J. Atmos. Sci.,* **47,** 856–869.

Holton, J. R., 1992: *An Introduction to Dynamic Meteorology.* 3d ed. Academic Press, 511 pp.

Hoskins, B. J., and P. J. Valdes, 1990: On the existence of storm tracks. *J. Atmos. Sci.,* **47,** 1854–1864.

——, and T. Ambrizzi, 1993: Rossby wave propagation on a realistic longitudinally varying flow. *J. Atmos. Sci.,* **50,** 1661–1671.

[5] Unlike for the sharp and strong PV gradient associated with a subtropical jet, the *transient,* sharp PV gradients associated with the polar-front jet (Swanson 2000) are a manifestation of barotropically decaying eddies.

Kim, H.-K., and S. Lee, 2001a: Hadley cell dynamics in a primitive equation model: Part I. Axisymmetric flow. *J. Atmos. Sci.,* **58,** 2845–2858.

——, and S. Lee, 2001b: Hadley cell dynamics in a primitive equation model: II. Nonaxisymmetric flow. *J. Atmos. Sci.,* **58,** 2859–2871.

Lee, S., 1997: Maintenance of multiple jets in a baroclinic flow. *J. Atmos. Sci.,* **54,** 1726–1738.

Lindzen, R. S., 1993: Baroclinic neutrality and the tropopause. *J. Atmos. Sci.,* **50,** 1148–1151.

——, and A. Y. Hou, 1988: Hadley circulations for zonally averaged heating centered off the equator. *J. Atmos. Sci.,* **45,** 2416–2427.

Palmén, E., 1954: Über die atmosphärischen Strahlströme. Meteor. Abhandl., Institute of Meteorology and Geophysics, Freien University, 35–50.

——, and C. W. Newton, 1969: *Atmospheric Circulation Systems.* International Geophysics Series, Vol. 13, Academic Press, 603 pp.

Panetta, R. L., 1993: Zonal jets in wide baroclinically unstable regions: Persistence and scale selection. *J. Atmos. Sci.,* **50,** 2073–2106.

——, and I. M. Held, 1988: Baroclinic eddy fluxes in a one-dimensional model of quasigeostrophic turbulence. *J. Atmos. Sci.,* **45,** 3354–3365.

Peixoto, J. P., and A. H. Oort, 1992: *Physics of Climate.* American Institute of Physics, 520 pp.

Penland, C., and P. D. Sardeshmukh, 1995: The optimal growth of tropical sea surface temperature anomalies. *J. Climate,* **8,** 1999–2024.

Riehl, H., 1962: Jet streams of the atmosphere. Tech. Rep. 32, Dept. Atmospheric Science, Colorado State University, 177 pp.

Schneider, E. K., 1977: Axially symmetric steady-state models of the basic state for instability and climate studies. Part II: Nonlinear calculations. *J. Atmos. Sci.,* **34,** 280–296.

——, and R. S. Lindzen, 1977: Axially symmetric steady-state models of the basic state for instability and climate studies. Part I. Linearized calculations. *J. Atmos. Sci.,* **34,** 263–279.

Simmons, A. J., and B. J. Hoskins, 1978: The life cycles of some nonlinear baroclinic waves. *J. Atmos. Sci.,* **35,** 414–432.

——, and ——, 1980: Barotropic influences on the growth and decay of nonlinear baroclinic waves. *J. Atmos. Sci.,* **37,** 1679–1684.

Sun, D.-Z., and R. S. Lindzen, 1994: A PV view of the zonal mean distribution of temperature and wind in the extratropical troposphere. *J. Atmos. Sci.,* **51,** 757–772.

Swanson, K. L., 2000: Stationary wave accumulation and the generation of low-frequency variability on zonally varying flows. *J. Atmos. Sci.,* **57,** 2094–2104.

——, P. J. Kushner, and I. M. Held, 1997: Dynamics of barotropic storm tracks. *J. Atmos. Sci.,* **54,** 791–810.

Thompson, D. W. J., S. Lee, and M. P. Baldwin, 2002: Atmospheric processes governing the Northern Hemisphere annular mode/North Atlantic Oscillation. *The North Atlantic Oscillation: Climatic Significance and Environmental Impact, Geophys. Monogr.,* No. 134, Amer. Geophys. Union, 81–112.

Thorncroft, C. D., B. J. Hoskins, and M. E. McIntyre, 1993: Two paradigms of baroclinic wave life-cycle behavior. *Quart. J. Roy. Meteor. Soc.,* **119,** 17–55.

Whitaker, J. S., and P. D. Sardeshmukh, 1998: A linear theory of extratropical synoptic eddy statistics. *J. Atmos. Sci.,* **55,** 237–258.

Williams, G. P., 1979: Planetary Circulations: 2. The Jovian quasi-geostrophic regime. *J. Atmos. Sci.,* **36,** 932–968.

Zhang, Y., and I. M. Held, 1999: A linear stochastic model of a GCM's midlatitude storm tracks. *J. Atmos. Sci.,* **56,** 3416–3435.